Toward Wearable Wireless Thermometers for Internal Body Temperature Measurements

3 AUTHORS, INCLUDING:

Parisa Momenroodaki

University of Colorado Boulder

12 PUBLICATIONS   **5** CITATIONS

Toward Wearable Wireless Thermometers for Internal Body Temperature Measurements

Zoya Popovic, Parisa Momenroodaki, and Robert Scheeler

ABSTRACT

This article overviews the motivations and challenges for non-invasive wireless measurements of internal human body temperature. Microwave radiometry is an attractive method for internal thermometry, with the possibility of a wearable device that can continuously monitor temperature inside body tissues in different parts of the body, store the data, and transmit it to a digital medical record. Currently, there are a limited number of available device solutions, and they are usually not wearable or wireless. Here we discuss a possible path to implementing such a thermometer, with some initial results demonstrating about 0.2 K measurement sensitivity, and a difference between the maximal and minimal error w.r.t. a thermocouple measurement of 0.5 K. Several probes for multi-band radiometers are also presented at frequencies of 410 MHz, and 1.4, 2.7, and 4.9 GHz. The main challenges of RF interference, sensitivity, calibration, spatial resolution, miniaturization, and probe design are discussed.

INTRODUCTION

There are a number of health-related applications, ranging from monitoring and diagnostics to therapy, which benefit from the knowledge of internal (core) body temperature. Generally, the external (skin) temperature differs from the temperature of internal tissues inside a human body by as much as 2.5 K, and also varies during the day [1]. In a number of disorders, this temperature difference changes and is not easy to measure externally. For example, long durations of exercise in heat conditions, such as in the case of athletes or soldiers under heavy training, can provoke brain heating, leading to premature fatigue and even death. Cancer cells can have increased temperatures, as can inflamed tissues such as joints of arthritis patients. Sleeping disorders are accompanied by changes in the circadian cycle, which are in turn related to changes in phase and amplitude of periodic core body temperature variations. Infants suffering from hypoxia-ischemia have an elevated brain temperature, and if detected can be effectively treated by hypothermic neural rescue [2]. In addition to diagnostics, therapy can be assisted by internal temperature monitoring, for example, in hyperthermia for cancer treatment and clinical high-intensity focused ultrasound (HIFU) for noninvasive therapy, where the knowledge of local temperature increase would be useful. A number of other interesting applications are discussed at the end of this article.

Existing methods for measuring core body temperature include invasive methods such as rectal probes, gastro-intestinal (ingestible) sensors [3], and surgically inserted thermometers. Ingestible sensors are short-range wireless devices that measure the temperature somewhere in the digestive tract for a limited time while the device is in the body. Magnetic resonance imaging (MRI) can be used for measuring temperature distribution with high spatial resolution, but is very expensive and not portable. With current trends to personalize medicine with wearable wireless sensors, there is a need for continuous temperature monitoring devices in different parts of the body (e.g., brain, heart), as illustrated in Fig. 1. Here, a wearable adhesive device on, say, the sternum continuously measures the temperature of the aorta (heart); the data is digitized, stored, and transmitted wirelessly to a digital medical record. The temperature is measured by a microwave radiometer.

All materials at non-zero temperatures emit electromagnetic radiation over all frequencies, governed by the black-body laws of physics. Microwave radiometry is a passive measurement of the black-body radiated power, which can indirectly give a measure of temperature. The black-body curve, which quantifies the power spectral density per solid angle as a function of frequency, has a peak that shifts as a function of object temperature. Some characteristic examples are shown in different colors in Fig. 1, for example, the 3 K cosmic background peaks in the microwave region, while the 6500 K Sun emission peaks in the visible part of the electromagnetic spectrum.

Human body temperature is normally around 37°C (310 K), so the peak of the radiation is in the infrared part of the electromagnetic spectrum (red line in Fig. 1). However, the wave penetration depth depends on electromagnetic

Zoya Popovic and Parisa Momenroodaki are with the University of Colorado, Boulder.

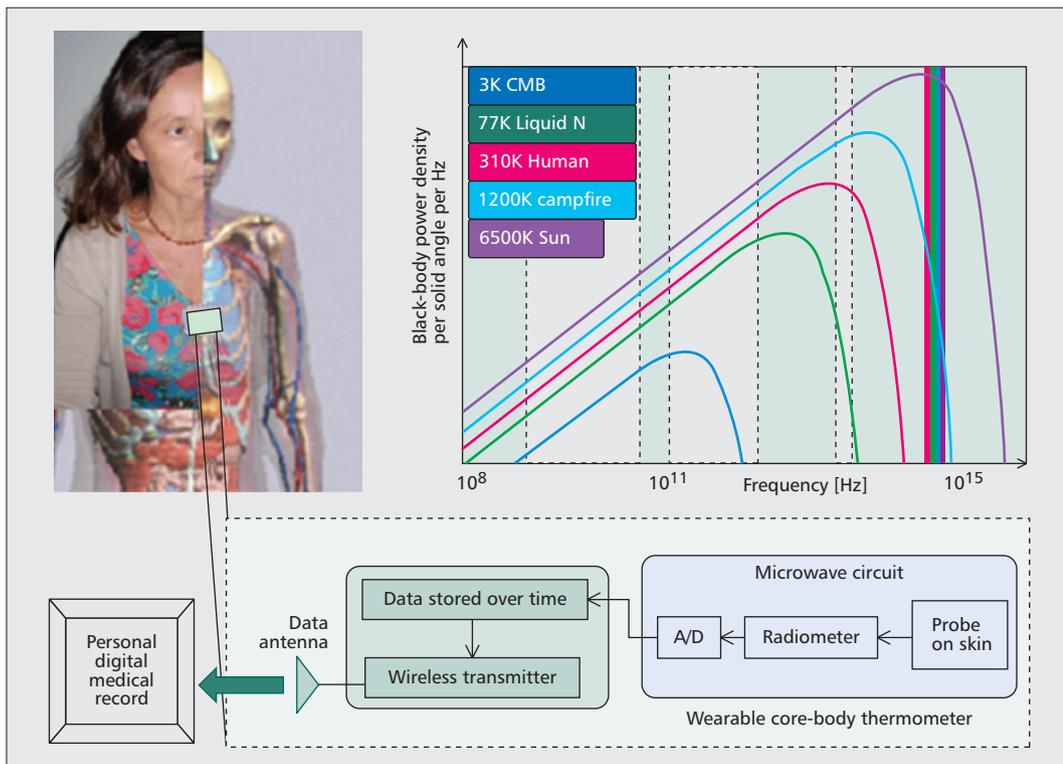*Robert Scheeler is with National Instruments.*

Figure 1. Illustration of a non-invasive external wireless device for core body thermometry. A wearable adhesive device on the sternum continuously measures temperature; the data is digitized, stored, and transmitted wirelessly to a digital medical record. The radiometer measures power radiated by tissues due to black body radiation. The plot shows the black-body power spectral density per solid angle as a function of frequency: 3 K cosmic background (blue); 77 K liquid nitrogen (green); 310 K human body (red); 1200 K fire (turquoise); and 6500 K Sun (pink), which peaks in the visible part of the spectrum.

properties of the material (e.g. conductivity) and on frequency, and is for plane waves given by the textbook skin-depth formula. At infrared frequencies, the waves do not penetrate beyond the top skin layer of the body, so thermal images obtained by IR cameras show surface temperature only. At millimeter-wave frequencies, the penetration depth is limited to the top skin layer and can be used for surface temperature monitoring, such as in the case of surface burns. Lower microwave frequencies around 1 to 4 GHz, however, have penetration depths in tissues on the order of centimeters. However, these frequencies are not at the peak of the 310-K black-body curve, but rather in the "tail," implying very low radiated power densities. This means that the design of radiometer electronics in Fig. 1 has two big challenges:

• Sensitivity, or minimal detectable temperature difference
• RF interference mitigation

The latter challenge is due to the ever increasing use of the electromagnetic spectrum by wireless communications and sensing. Other challenges for this application, discussed below, include the need for three-dimensional spatial resolution, complexity of human tissues, and potential requirement to measure both relative and absolute temperature profiles.

It is therefore not surprising that there has been limited research in microwave core-body thermometry, mainly limited to infant brain temperature measurements (e.g. [2, 4]) and for mon-itoring astronaut temperature in space suits [5]. However, in these cases typically the environment is shielded, or relatively large shielded probes are used, resulting in non-wearable devices. An interesting commercial product, with a focus on clinical detection of breast cancer, has a resolution of 0.2 K, uses a handheld shielded probe, and has a mass of 4 kg [6]. None of the above approaches are wireless or intended for monitoring core body temperature continuously over long periods of time. The remainder of this article presents a path to such a device.

MICROWAVE THERMOMETER OPERATION

The radiometer device from Fig. 1 can be implemented in a variety of architectures, which are used in many disciplines such as radio astronomy [7], terrestrial remote sensing [8], fire monitoring, food , and so on. In most of these applications, the object of unknown temperature is in the far field of the antenna, which receives plane waves radiated by the object. In the core body thermometry case, however, the power radiated by the tissues is received by a probe situated in the near field, on the skin. Below the dry skin layer (epidermis) is a wet layer of skin (dermis) and a layer of fat (hypodermis), followed by muscle and bone. The different layers are characterized by significantly different electrical properties (i.e., permittivity and conductivity).
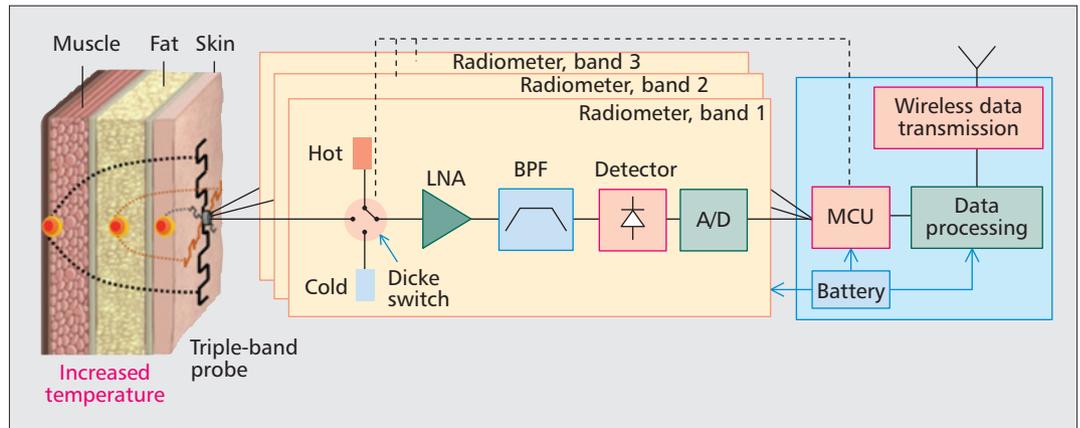
Figure 2. Block diagram of a 3-frequency internal body temperature measurement system. The power received from tissue layers by the narrowband probes is coupled to the Dicke radiometer circuits, which consist of a switch that is required for calibration, a low-noise amplifier (LNA) followed by band-pass filters, and a diode detector circuit. The hot and cold loads are used for continuous temperature calibration of the radiometer. The detector output is a DC voltage which can be integrated over time to increase the signal-to-noise ratio (SNR). This output is digitized, processed, and transmitted through a wireless unit. A micro-controller unit (MCU) controls the radiometer switches enabling phase-sensitive detection of the very low human black-body power levels.

Consider the case of a local heating of tissue under a few layers. The radiometer measures total power received from all the layers, and in order to determine the position of increased temperature, several frequencies corresponding to different penetration depths are used. For example, a five-band radiometer from 1 to 4 GHz is proposed in [2] to measure infant brain temperature. In this case, a broad frequency range (3 GHz bandwidth) was used to collect more power by integrating over frequency using a relatively large shielded device.

In the case of a wearable miniaturized radiometer, any electromagnetic interference (EMI) will result in errors in the estimation of the temperature. Figure 2 shows a more detailed block diagram of a multi-band radiometer that uses narrowband probes designed at three frequencies to sense depth profile. Each probe couples the received power to a Dicke radiometer circuit [7, 8], designed for the specific frequency, with multiple stages of filtering that help mitigate EMI. The DC voltage output of each radiometer is digitized, and the data can be processed to estimate the temperature increase and the location. The measured temperature and spatial resolution depend on radiometer sensitivity and linearity, as well as the algorithm used to take into account tissue layer radiation.

The choice of frequencies needs to take into account both EMI and penetration depth into tissues, as well as probe size. In this work, we use frequencies protected for radio-astronomy and space research: 410 MHz (emissions prohibited by both the FCC and ITU from 406.1–410 MHz), 1.4 GHz (1.4–1.427 GHz), and 2.7 GHz (2.65–2.7 GHz). Other options include the 4.8–5 GHz protected band, but the penetration depth is small (less than 1 mm), and this would be useful only for comparing to other surface thermometers. In the 410 MHz band the wavelength is larger, resulting in the need to miniaturize the probe.

In a narrow measurement frequency bandwidth (B), the power received can be approximated by the simple thermal (white) noise expression $P = kT_AB$, where T_A is the antenna temperature, which depends on both the physical temperature and the antenna directional parameter, which describes the power an antenna receives from a cone described by spherical angles (θ, ϕ). Once the power is measured by the radiometer, a model is needed for the tissue stack-up to determine the temperature distribution. This has been done with near-field weighting functions estimated from some type of electromagnetic simulation, such as finite diference time domain (FDTD), finite element method (FEM), and semi-analytical [9]. Each weighting function defines the contribution from a differential volume (e.g., layer of tissue) to the overall antenna temperature. The weighting functions, which depend on the tissue stack-up and probe design, are found as the power absorption rate, which is the dissipated power in a certain volume, normalized to the total dissipated power [9].

The dielectric properties of tissues have been widely studied, and the standard resource is a series of articles from S. Gabriel and C. Gabriel that include a literature survey, measurements, and models for various human tissues. For the designer, there are several resources where these tissue properties are available. For dielectric properties of various tissues in the frequency range of 10 Hz to 100 GHz, "An Internet Resource for the Calculation of the Dielectric Properties of Body Tissues" from the Italian National Research Council is a great resource. Additionally, the "Tissue Properties Database" from the IT'IS Foundation has not only the dielectric properties of the tissues, but also physical properties such as density and thermal conductivity. IT'IS also has a virtual population of body models [10] that can be used to estimate tissue thick-
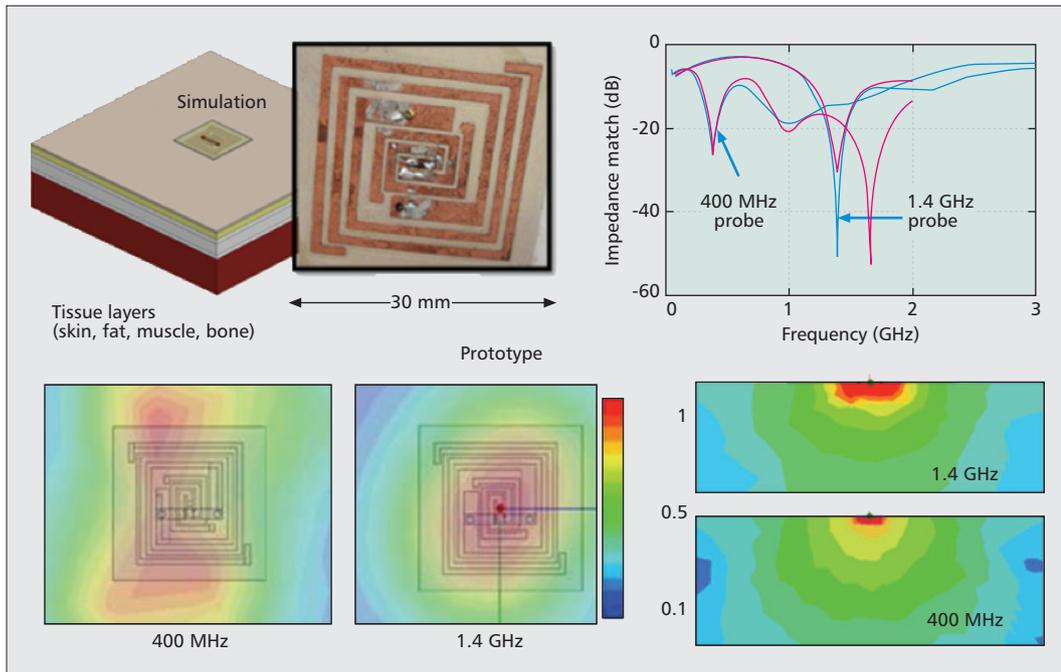
Figure 3. Simulated and implemented dual-frequency wearable antenna probe, with two feed lines that can be connected to a 406-MHz and 1.4-GHz radiometer. Simulated and measured results for the reflection coefficient when placed on the sternum (blue-measured; red-simulated). The bottom plots show simulated specific absorption rate (SAR) at the two frequencies from top and side. Each plot is normalized to the peak value at that layer in the tissues.

The SAR was determined by electromagnetic field simulations at the interface between the heart and cortical bone. While SAR is usually used to determine if tissues are absorbing power from a source, because of reciprocity between black-body emission and absorption, it can also give an estimate of how much power is emitted.

nesses for different people to account for inter-subject variability. The models can be inserted in the full-wave FDTD simulation tool SEM-CAD-X by Speag to calculate, for example, specific absorption rate (SAR), defined as power absorbed by unit mass of a tissue.

Although the temperature dependence and detailed frequency dependence of tissue parameters are important for design, here it will suffice to point out that the dielectric constant at 1 GHz varies from 40 (epidermis) to 5.5 (fat) and 55 (muscle), while the conductivity varies from 0.9S/m to 0.05S/m and 0.98S/m, respectively. Knowledge of the dielectric properties is essential for design of the probe, frequency selection, and inversion of the radiometric observations to determine the physical temperature of the tissues.

PROBE DESIGN

The probe (near-field antenna) design is envisioned to be on a thin flexible substrate and in direct contact with the skin, or possibly using a thin gel impedance-matching layer. A dual frequency probe designed for placement on the human sternum for the application of determining the temperature of the human heart is shown in Fig. 3. The tissue stack is assumed to be 1.2 mm skin/4 mm fat/2 mm cortical bone/7 mm cancellous bone/2 mm cortical bone/heart. The probe consists of two dipoles that are folded in a spiral fashion to reduce the size at the lower frequency. The high-frequency probe is nested in the low-frequency probe to ensure that power dissipation patterns are spatially collocated. The probe was printed on Rogers 3010 25-mil thick board material, which is somewhat flexible. Two separate feeds cover the 406.1–410 MHz and 1.4–1.427 GHz bands allocated for radio-astronomy. The design was first simulated with a model for the human sternum comprising complex permittivity layers to simulate human tissues. The simulation assumes an infinite transverse extent for the layers of tissues.

The full-wave electromagnetic simulation tool HFSS from Ansys was used to determine the input impedance and power dissipation pattern, and the simulation environment and comparison to measured results are shown in Fig. 3. The measured data for the impedance match on the human sternum just above the heart is obtained with a network analyzer. The agreement between measured and simulated data shows that this method can be effectively used for probe design. The far-field pattern of the probe was measured at 1.4 GHz in a non-shielded environment and confirmed that very little radiation is received from directions outside of the body.

The specific absorption rate (SAR) was determined by electromagnetic field simulations at the interface between the heart and cortical bone. While SAR is usually used to determine if tissues are absorbing power from a source, because of reciprocity between black-body emission and absorption, it can also give an estimate of how much power is emitted. The SAR normalized to the peak value is shown in Fig. 3 for the two frequencies and for two cross-sections. It can be seen from the SAR plots close to the surface that the maximum occurs directly below the feed. Further into the tissues, however, the maximum begins to occur in the center of the entire probe footprint.

Figure 4. Photograph and measured vs. simulated impedance match for a three-frequency probe designed to be placed on the abdomen (as measured).

A three-frequency probe (1.4, 2.7, and 4.9 GHz) placed on the human abdomen assuming a 1-mm thick skin layer, 2-mm thick fat layer, and infinitely thick muscle layer was also designed, as shown in Fig. 4 [9]. The probes are designed to be as collocated as possible so that their power dissipation patterns coincide spatially in the tissue stack. For this reason the two lower frequency probes are bent as shown in the photograph. The probes are made on a Rogers RO-4350B 0.762-mm thick substrate with a permittivity of 3.66, and each dipole is fed with a microstrip tapered balun. The dipoles are measured *in vivo* on the abdomen with one of the authors serving as a volunteer. The measured results compared to high-frequency structure simulator (HFSS) simulations for the three probes demonstrate a good impedance match (better than –15 dB) for each probe at the respective design frequencies.

The simulated normalized weighting functions were calculated for this probe, and in each case, over 50 percent of the power accepted into the probe is dissipated in the 1-mm thick skin layer. The lowest frequency probe dissipates the most power in the muscle. Less than 10 percent of the power is dissipated in the fat layer, and this percentage decreases with increasing frequency in this particular case.

RADIOMETER DESIGN AND PERFORMANCE

The ideal total power radiometer minimal detectable temperature difference is given by

$$\Delta T = \frac{T_{sys}}{\sqrt{B\tau}} = \frac{T_A + T_{rec}}{\sqrt{B\tau}}$$

where T_{sys} is the system noise temperature (including antenna and receiver), B is the bandwidth of the receiver/antenna system, and τ is the integration time over which the power is received. T_A and T_{rec} are the antenna and receiver temperature, respectively. The above formulas are valid for a black body that has an emissivity of 1, and for a body that has emissivity $e(\theta, \varphi)$, the temperature is modified to

$$T_{eff}(\theta, \varphi) = e(\theta, \varphi)T.$$

As seen from the above formulas, the minimal detectable temperature is a trade-off between system temperature (which should be as low as possible), bandwidth (more bandwidth implies more power and better SNR) and integration time (longer integration time results in lower noise floor and thus improves the SNR). For a wearable radiometer that generally does not operate in a shielded environment, the bandwidth B cannot be large, and therefore, we expect to have to minimize the system noise temperature and increase integration time. The system noise temperature will be dominated by the switch and LNA connected to the probe.
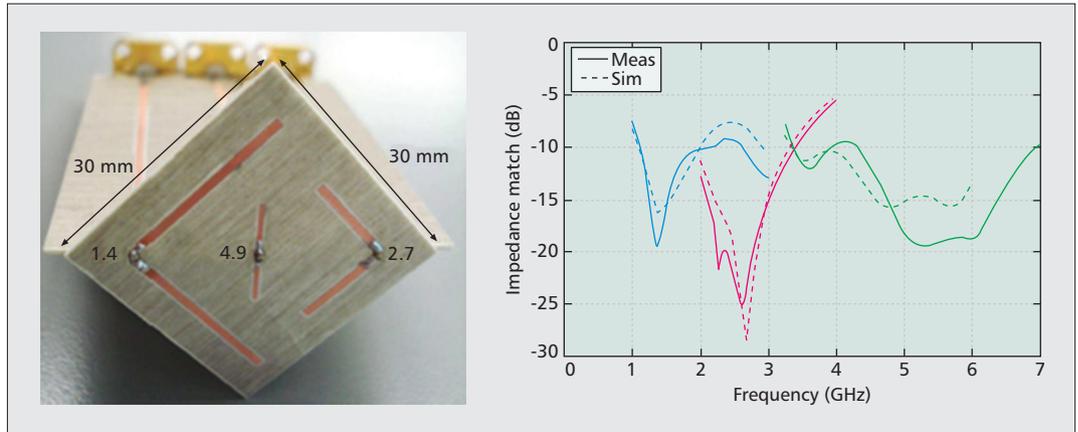
A highly sensitive receiver must be calibrated to associate the output voltage to a physical temperature. The receiver can be measured with two known temperature inputs to get a linear calibration relationship of voltage to temperature, as shown in Fig. 2. The temperature differences are obtained by "hot" and "cold" temperature loads [7].

In the literature, there have been a number successful demonstrations of CMOS-based radiometers in the microwave frequency range for applications, such as, e.g. fire detection [11]. Such miniaturization is beneficial to the core body measurement problem, but would require improved sensitivity and calibration.

For initial proof-of-principle results, we have designed two radiometers at 1.4 and 2.7GHz based on off-the-shelf components [12], using the following design procedure:
• Choose the frequencies of operation based on low interference (quiet protected band) and penetration depth.
• Design a detector matched to 50Ω for the selected frequency bands, e.g. using a Schottky diode matched with lumped surface-mount components.
• Based on expected tissue temperature variations and the thermal noise narrowband approximation $P = kTB$, where $k = 1.38 \times 10^{-23}$ J/K is the Boltzmann constant, T is the temperature in Kelvin, and B is the radiometer bandwidth, calculate the expected signal levels at the input of the radiome-
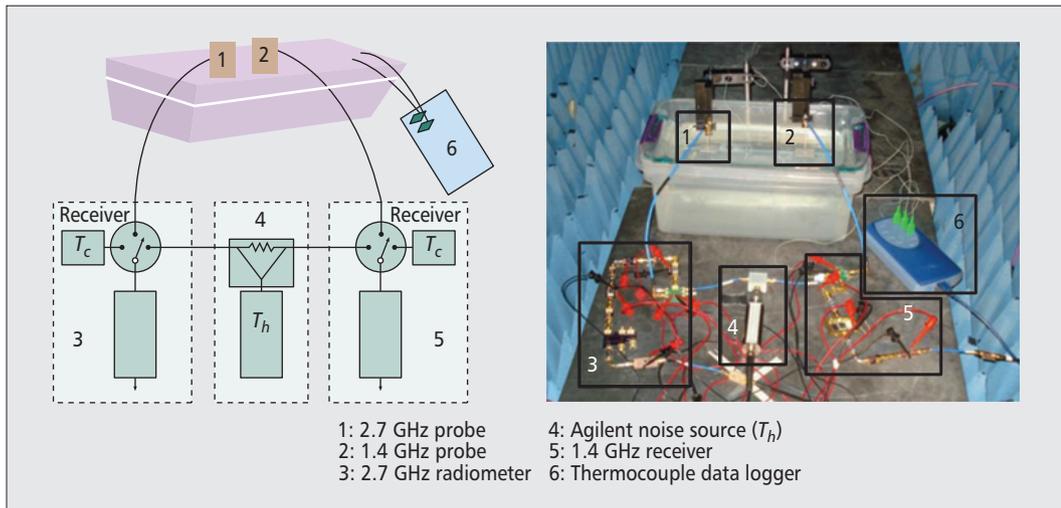
Figure 5. Photograph of block diagram (left) and measurement setup (right) used for two-frequency (1.4/2.7 GHz) measurement of a three-layer phantom consisting of a 10.3 mm thick layer of 42°C water (representing skin) above a 5-mm thick layer of glass (representing fat) and more than 5 cm of water (muscle) kept at room temperature. The top water layer temperature is monitored with a thermocouple. The data is recorded with a PicoTech data logger.

ter, for example, approximately –100 dBm at 1.4 GHz.
- Choose the desired power levels in the linear region of the square-law detector, giving the output power of the radiometer.
- Design the receiver front-end to have a gain that stays above the noise floor of the detector. This can be a combination of LNAs and filters, as shown in Fig. 2 with a single filter and amplifier. For the 1.4-GHz radiometer, a desired gain of $G = 45$ dB is calculated.
- Ensure that the noise figure of the system meets the design requirements for receiver sensitivity by proper component selection. For a desired noise figure of $NF = 3$ dB, in the 1.4-GHz radiometer case, the block diagram from Fig. 2 is implemented using the following components. The Dicke switch is a Hittite HMC345LP3 component with a noise figure of 2 dB and insertion loss of 2 dB. The LNA is implemented with two stages: the first stage is a MiniCircuits RAMP-33LN device with a noise figure of $NF = 1$ dB and gain of $G = 16$ dB 1 dB, followed by a MiniCircuits VBFZ-1400 bandpass filter with a noise figure of 2 dB and insertion loss of 2 dB. This is followed by a second-stage LNA, which is a MiniCircuits TAMP component with $NF = 0.6$ dB and $G = 32$ dB, and a second bandpass filter.

The 2.7-GHz radiometer is implemented using the same procedure and with similar off-the-shelf components. The radiometers are connected to probes similar to the ones presented in the previous section and tested by measuring a three-layer phantom consisting of a 10.3-mm thick layer of 42°C water (representing skin) above a 5-mm thick layer of glass (representing fat) and more than 5 cm of water (muscle), as shown in Fig. 5. The latter is kept at room temperature, and the measured and estimated tem-

peratures are shown in Fig. 6. The temperature inversion process is done with one of several possible estimation techniques. It can be seen that the top layer thermocouple measurement, $T_{v1,fit}$ (fitted to the exponential equation because of different sampling rate from the measurements), and the radiometric estimate, T_{v1}, have less than 2°C absolute temperature error. The same error can be seen in the bottom layer thermocouple measurement, $T_{v3,fit}$, and the radiometric estimate, T_{v3}. Although a 2°C error might seem large if absolute temperature is required, there are a number of applications that require only relative temperature (e.g., circadian rhythm monitoring) [13]. In this case, it is important that the error remain constant over time. For the fitted data, the difference between the maximum and minimum error in the top and bottom layers is 0.5°C and 0.4°C, respectively.

Conclusions

In summary, this article briefly reviews the motivation and challenges for internal body temperature measurements, and presents a possible non-invasive approach with an external device that can be wearable and wireless. In addition, the device can be used for measuring internal temperature of any part of the body, once properly calibrated. Measurements can be done over long periods of time without interfering with daily life. The advantages of this method in diagnostics and therapy are not limited to those mentioned in the introduction. Examples include early malignant tumor detection due to increased tumor temperature compared to surrounding tissues; monitoring drug delivery for cancer treatment; detection of vesicoureteral reflux in children and quantification of in vivo inflammation in atherosclerotic plaques in vascular pathology; monitoring temperature of transplant organs; monitoring the circadian cycle; monitoring brain temperature in acute brain injuries and
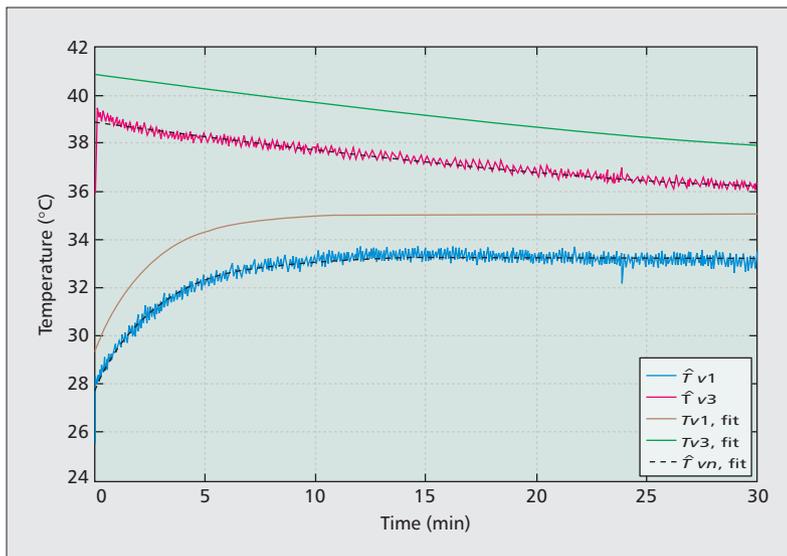
Figure 6. Two-frequency measurement results above the three-layer phantom of water (skin), glass (fat), and water (muscle). The top layer thermocouple measurement, $T_{v1,fit}$, and radiometric estimate (T_{v1}) has less than 2°C absolute temperature error. The same error can be seen in the bottom water layer thermocouple measurement, $T_{v3,fit}$, and its radiometric estimate (T_{v3}). The dashed line ($T_{vn,fit}$) is an exponential fit to the estimate.

during electrical stimulation to prevent tissue damage; and tracking of abnormal flow of fluids (extravasation) such as urine or antineoplastic drugs. Applications other than medical include accurate determination of core body temperature at the scene of a crime or in an autopsy to determine postmortem interval in forensics, profiling food temperature during transportation and manufacturing, and furthering the study of endothermic and ectothermic animal survival mechanisms in cold conditions.

The challenges associated with designing a manufacturable and cost-effective wearable wireless radiometer include susceptibility to interference due to the very low levels of power emitted by the tissues. This can be mitigated by multiple stages of filtering in the probe and circuit design, but also by miniaturization of the probe and circuits. Another challenge is both radiometer and model calibration, given that each human is different and the electric properties of tissues vary. So far, limited work has been done on the temperature estimation for multi-frequency measurements of multi-layer structures, and additional estimation techniques need to be addressed to minimize biases in the estimated data. Finally, in some cases relative temperature measurements are sufficient, while in other cases absolute temperature is required. This is a more difficult measurement and would most likely require an independent known temperature source for additional calibration during measurements.

Although the microwave thermometer demonstrated in this article is not yet wireless and is implemented from commercial connectorized parts at this stage, miniaturization using several chips, and ultimately monolithic integration, is certainly possible. For example, the LNA, switch, detector, and cold noise source have all been demonstrated in GaAs

monolithic microwave integrated circuits (MMICs) with excellent performance. There are many LNA and switch IC examples, such as the TriQuint TQP3M9035 LNA with $NF = 0.66$ dB and $G = 16$ dB from 0.05 to 4 GHz, and the TQP4M0008 single-pole double-throw (SPDT) switch, which has a 0.3 dB insertion loss and greater than 20 dB isolation from 0.1 to 4 GHz [14]. We have also demonstrated a cold noise source GaAs MMIC with a noise temperature of less than 90 K from 1.3 to 1.5 GHz with a return loss greater than 28 dB [15], and these components can all be integrated in a single small chip. The back-end of the radiometer is amenable to standard complementary metal oxide semiconductor (CMOS) processes, or can be assembled from commercially available die. The ICs are small, and can be mounted and interconnected on the flexible substrate with the probe. The target goals are a total size of an adhesive bandage, a weight of a few ICs in addition to the 5 gr probe, and a power dissipation below 0.1 W.

In summary, this article presents an overview of microwave thermometry for internal body temperature measurements, along with a working radiometer that operates in two quiet bands (1.4 and 2.7 GHz). The probe is made on a flexible substrate, has very low mass, and is conformal. Measurements on a three-layer phantom show the feasibility of internal measurements at depths of several centimeters assuming uniform layers. It is shown that relative temperature differences can be measured with an error that is less than 0.5 K.

REFERENCES

[1] K. Kräuchi et al., "Functional Link between Distal Vasodilation and Sleep-Onset Latency?," *Amer. J. Physiology — Regulatory, Integrative and Comparative Physiology*, vol. 278, no. 3, 2000, pp. R741–R748.

[2] J. W. Hand et al., "Monitoring of Deep Brain Temperature in Infants Using Multi-Frequency Microwave Radiometry and Thermal Modelling," *Physics in Medicine and Biology*, vol. 46, no. 7, 2001, p. 1885.

[3] D. M. Wilkinson et al., "The Effect of Cool Water Ingestion on Gastrointestinal Pill Temperature," *Medicine & Science in Sports & Exercise*, vol. 40, no. 3, Mar. 2008, pp. 523–28.

[4] S. Jacobsen and P. Stauffer, "Multifrequency Radiometric Determination of Temperature Profiles in a Lossy Homogeneous Phantom Using A Dual-Mode Antenna with Integral Water Bolus," *IEEE Trans. Microwave Theory and Techniques*, vol. 50, no. 7, July 2002, pp. 1737–46.

[5] Q. Bonds, T. Weller, and P. Herzig, "Towards Core Body Temperature Measurement via close Proximity Radiometric Sensing," *IEEE Sensors J.*, no. 99, 2011, p. 1.

[6] http://www.resltd.ru/eng/literature/index.php?lit_page=biblio.

[7] J. D. Kraus, *Radio Astronomy*, 2nd ed., Cygnus-Quasar Books, 1976, pp. 1–3, 20–23, 66.

[8] F. T. Ulaby, R. K. Moore, and A. K. Fung, *Microwave Remote Sensing: Active and Passive, Volume 1: Microwave Remote Sensing Fundamentals and Radiometry*, Artech House, 1981, pp. 1–3, 20–24, 93–94, 112, 122–23.

[9] R. Scheeler, E. Kuester, and Z. Popovic, "Sensing Depth of Microwave Radiation for Internal Body Temperature Measurement," *IEEE Trans. Antennas and Propagation*, vol. 62, no. 3, Mar. 2014.

[10] IT'IS, "The Virtual Population," 2013, http://www.itis.ethz.ch/services/anatomical-models/overview/.

[11] F. Alimenti et al., "System-on-Chip Microwave Radiometer for Thermal Remote Sensing and Its Application to the Forest Fire Detection," *15th IEEE Int'l. Conf. Electronics, Circuits and Systems*, Aug. 31–Sept. 3, 2008, pp.1265, 1268.

[12] R. Scheeler, P. Momenroodaki, and Z. Popovic, "Microwave Radiometry for Internal Body Temperature Monitoring" *36th IEEE Engineering in Medicine and Biology Conf.*, Chicago, IL, Aug. 2014.

[13] N. E. Rosenthal *et al.*, "Effects of Light Treatment on Core Body Temperature in Seasonal Affective Disorder," Biological Psychiatry, vol. 27, no. 1, 1990, pp. 39–50.

[14] http://www.triquint.com/

[15] R. Scheeler and Z. Popovic, "A 1.4 GHz MMIC Active Cold Noise Source," *IEEE Compound Semiconductor IC Symp. Digest*, Monterey, CA, Oct. 2013, pp.1–4.

BIOGRAPHIES

ZOYA POPOVIC [S'86, M'90, SM'99, F'02] received her Dipl.Ing. degree from the University of Belgrade, Serbia, Yugoslavia, in 1985, and her Ph.D. degree from the California Institute of Technology, Pasadena, in 1990. Since 1990, she has been with the University of Colorado at Boulder, where she is currently a Distinguished Professor and holds the Hudson Moore Jr. Endowed Chair in the Department of Electrical, Computer and Energy Engineering. In 2001/03 and 2014, she was a visiting professor with the Technical University of Munich, Germany, and ISAE in Toulouse, France, respectively. She was elected a Foreign Member of the Serbian Academy of Sciences and Arts in 2006. Since 1991, she has graduated 50 Ph.D. students, and currently leads a group of 15 doctoral students and 4 post-doctoral fellows. Her research interests include high-efficiency transmitters for radar and communication, low-noise and broadband microwave and millimeter-wave circuits, antenna arrays, wireless powering for batteryless sensors, and medical applications of microwaves such as microwave core-body thermometry and traveling-wave MRI. She was the recipient of the 1993 and 2006 IEEE MTT-S Microwave Prizes for the best journal papers. She received the 1996 URSI Issac Koga Gold Medal, was named an NSF White House Presidential Faculty Fellow in 1993, and received the German Humboldt Research Award in 2000. She won the 2001 Hewlett-Packard(HP)/American Society for Engineering Education(ASEE) Terman Medal for combined teaching and research excellence, and was named IEEE MTT Distinguished Educator in 2013.

PARISA MOMENROODAKI [S'13] received her B.Sc. degree in electrical engineering from Shariaty University, Tehran, Iran, in 2008. She received her M.S. degree from Amirkabir University of Technology, Tehran, in 2011 and worked as an RF research engineer at Faramoj. She is currently pursuing a Ph.D. at the University of Colorado in the area of microwave radiometry for medical applications. Her research interests include passive and active sensing, microwave active circuits, antennas, and mixed-signal electronics.

ROBERT SCHEELER (S'12) received his B.S. degree in electrical engineering at North Dakota State University in 2008, and his M.S. and Ph.D. degrees in electrical engineering at the University of Colorado at Boulder in 2011 and 2013, respectively. He is currently a PDK development engineer at National Instruments Applied Wave Research, Louisville, Colorado. His research interests include low-noise receivers, on-chip noise calibration standards, monolithic microwave integrated circuit design, wireless energy harvesting, and non-invasive core body temperature measurement using microwave radiometers.